

FATIGUE CRACK GROWTH IN PARTICLE-REINFORCED METAL MATRIX COMPOSITES

FERNAND ELLYIN
NOVACOR/NSERC Senior Industrial Research Chair
Department of Mechanical Engineering
University of Alberta
Edmonton, Alberta, Canada T6G 2G8

ABSTRACT

The fatigue crack growth behaviour of particle-reinforced metal matrix composites is presented. Different types of damage caused by cyclic loading is identified first. It is shown that the growth of initiated short cracks is microstructure sensitive and the growth may cease depending on the level of applied far field stresses. The inability of reinforced particles to resist a long crack growth is explained based on an energy consideration of the crack extension. Various crack growth regimes are combined into a crack-phase diagram, relating the appropriate boundaries with the overall properties of the composite. It is demonstrated that the particle size influences the stress distribution in front of the crack and the crack-tip displacement.

KEY WORDS

Alumina, aluminum, composite, crack growth rate, crack phases, fatigue crack, metal matrix, particle-reinforced, short crack.

INTRODUCTION

The industrial use of particle-reinforced metal matrix composites (PMMC's) is steadily increasing, especially in the aeronautic and automobile industries. Compared with their fibre reinforced counterparts, the production cost of PMMC's is much lower, and most of the present manufacturing techniques of metals and alloys can be easily adapted to PMMC's.

The ease of production and the resulting isotropic mechanical properties, place a limit on the amount of strengthening of the matrix alloy. In particular, ductility of PMMC's is considerably reduced with the increased particle volume fraction (Llyod, 1995). This in turn imposes a restriction on the wider use of PMMC's, especially in those applications where more ductility is desired. The aforementioned reduced ductility requires that the resistance of PMMC's to crack growth be properly understood before they are used in critical components.

It is the objective of this paper to discuss the resistance of PMMC's to short and long crack growth. The crack initiation sites in smooth specimens will be first identified, followed by an investigation of short crack growth and trapping. The behaviour of long cracks and the ineffectiveness of particles to influence the crack growth in the intermediate stress intensity range (above the threshold stress intensity range) will then be discussed. An analysis based on the energy required to extend a crack, will be subsequently presented to rationalized the above

observed behaviour. Finally, a crack growth phase diagram for PMMC's is described, illustrating various regimes of crack growth in an applied stress versus crack length coordinates. This diagram is of interest to materials and mechanical designers.

Material Specification

The experimental results to be presented here are for an alumina (Al_2O_3) particle-reinforced 6061 aluminum alloy. The material was heat treated to T6 condition. The average alumina particle size was $12\ \mu\text{m}$ with particles varying from 5 to $80\ \mu\text{m}$ in diameter. They were, however, smaller than the average grain size of the aluminum alloy matrix. The particles in general were angular, containing sharp corners and edges. The volume fraction of particles were 10 and 20%. The monotonic yield stress of the composite, σ_{yc} , varies with the particle volume fraction according to the following empirical formula (Duralcan 1993)

$$\sigma_{yc} = \sigma_{ym}(1 + f_v^\alpha)/C \quad (1)$$

where α and C are constants equal to 2.1 and 1.14, respectively for the $\text{Al}_2\text{O}_3/6061\ \text{Al}$, and σ_{ym} is the yield stress of 6061 Al matrix. The cyclic properties for a 20% particle volume fraction are: $\sigma'_{yc} \approx 350\ \text{MPa}$, with a fatigue limit of $\sigma_{fl} \approx 100\ \text{MPa}$. The elastic modulus of the composite, $E_c \approx 107\ \text{GPa}$, while that of the matrix is, $E_m \approx 70\ \text{GPa}$. The matrix cyclic yield stress $\sigma'_{ym} \approx 280\ \text{MPa}$.

Observed Microstructural Damage

Microscopic observations of shallow notch specimens with deeply electro-polished surfaces, and subjected to cyclic loading, revealed three types of microstructural damage (Li and Ellyin, 1996):

(i) **Particle debonding** where large particles are most likely to debond; (ii) **Particle fracture** which occurs under high stress amplitude, and (iii) **Matrix cracking** that is often induced by the first two types of damage. This type of cracking generally occurs at a later stage of damage development. Thus, particles are generally the initiation sites of short cracks.

Once a short crack is initiated, its growth is highly influenced by the heterogeneous distribution of particles. In the PMMC's, particles are much stronger barriers than the grain boundaries in metals and alloys. In the following we will discuss the behaviour of short and long cracks and the effect of local heterogeneity on the growth of these cracks.

SHORT CRACK BEHAVIOUR IN PMMC'S

Two characteristics distinguish the short crack behaviour in PMMC's. First, both growth direction and growth rate are dramatically affected by particles, especially the large ones. Second, the size of short cracks which exhibit microstructure-sensitivity is much longer than that

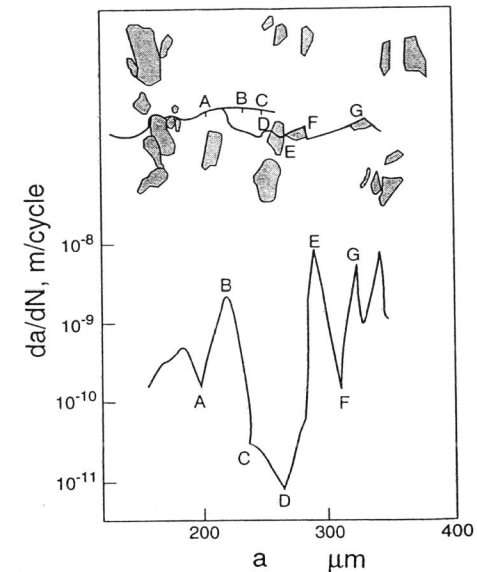


Fig. 1 Short crack path and its crack growth rate vs. crack length under a maximum cyclic stress of $\sigma_{max} = 110\ \text{MPa}$, $R = -0.35$

in metals and alloys. For example, Fig. 1 shows the growth of an initially short crack of $a_i \approx 120\ \mu\text{m}$ under a maximum stress of $\sigma_{max} = 110\ \text{MPa}$ ($\Delta\sigma = 150\ \text{MPa}$, $R \approx -0.35$). The crack extension up to three times the initial crack length is highly influenced by the particles as shown in the upper part of the figure, Li and Ellyin (1995a). The fracture of an average sized particle on the crack path plays a key role in maintaining the crack growth. A fractographic study shows that the plastic zone ahead of a short crack has a multiple slip character, Li and Ellyin (1995b).

The effect of a nearby particle on the stress/strain distribution in front of an advancing crack was investigated by a finite element analysis, Li and Ellyin (1994). Figure 2 shows the effect of a nearby particle on the stress distribution of an approaching short crack. Crack tip stress contours in the composite are plotted and compared with those in the matrix alloy under the same loading condition and geometry. It is seen that the presence of a particle in the crack path causes the maximum stress to displace from the crack tip to the particle. That is, the crack tip stress decreases, and the normal tensile stress at the particle increases, especially on the part facing the crack tip. Further more, there is an increase in the stress magnitude in the space between the two particle ahead of the short crack (Fig. 2).

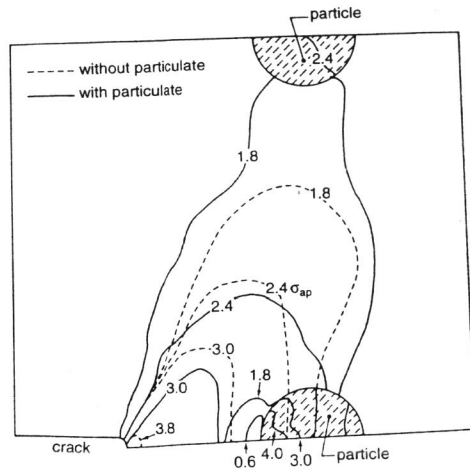


Fig. 2 Stress contours ahead of a short crack in $\text{Al}_2\text{O}_3/6061\text{A1}$ composite (solid lines) compared with the stress contours of the same length crack in 6061A1 alloy (dashed line) under the same loading condition. Applied stress is 60% of the composite yield stress, σ_{yc} .

The plastic zone size ahead of a crack is also affected by the presence of the particles. As the crack approaches a particle on its path, the plastic zone size decreases. Since the crack growth results from the damage caused by irreversible movement of dislocations in the cyclic plastic zone, the change in the crack tip plastic zone size and shape will promote a change in the crack growth as the crack approaches a particle (Li and Ellyin, 1994).

Figure 3 shows an example of a short crack growth and its arrest. Here an initial crack of length $a_i \approx 180 \mu\text{m}$ is subjected to a maximum stress of $\sigma_{\max} = 99 \text{ MPa}$ (about the fatigue limit of the material). The crack growth pattern follows the drastically varying rate usually observed in the short crack growth (cf. Fig. 1). In this case, however, after growing for about $100 \mu\text{m}$, the crack tip reaches a large particle and ceases to propagate. The local stress state is not high enough to fracture the particle.

From the foregoing discussion we can distinguish two regimes of short crack growth, one which has sufficiently high crack tip stress field to drive it passed the particle, and the second which is blocked by the particle(s). The latter is termed pre-cess short crack growth by Li and Ellyin (1995a).

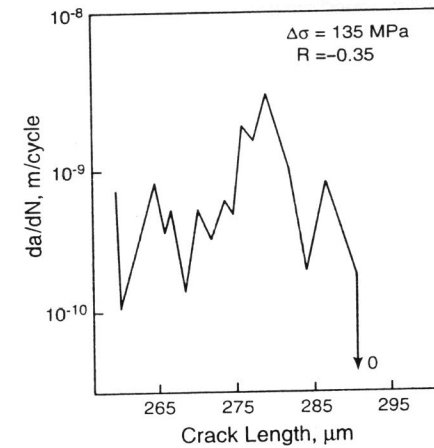


Fig. 3 A short crack growth and its arrest by a cluster of particles under applied $\sigma_{\max} = 99 \text{ MPa}$ with $R = -0.35$.

LONG CRACK GROWTH

The crack growth rate, da/dN , versus the maximum stress intensity factor, K_{\max} , for cracks longer than 3 mm is shown in Fig. 4, in a log-log scale, for a composite with 10% and 20% particle volume fraction and the matrix alloy. It is seen that in the intermediate stress intensity, $K_{\max} > 8 \text{ MPa(m)}^{1/2}$, all the data fall on a straight line with a narrow scatter band. This indicates that the growth rate in the intermediate K_{\max} (or ΔK) is independent of particles. However, in the near threshold region, there are three distinct growth curves for each material. The threshold stress intensity factor varies from $4.5 \text{ MPa(m)}^{1/2}$ for the matrix to $6.5 \text{ MPa(m)}^{1/2}$ for the 10% volume fraction composite to $7.5 \text{ MPa(m)}^{1/2}$ for that of 20%. Thus, the threshold stress intensity increases by about 44% for the first 10% particulate reinforcement and by about 22% for the next 10% reinforcement compared to the matrix threshold value. This is a fairly substantial increase in the threshold stress intensity which indicates an increased resistance to crack growth at the low (near threshold) values due to the presence of particles.

This type of behaviour has also been reported for silicon carbon particle-reinforced aluminum, e.g. see Shang and Ritchie (1989). The reason for the ineffectiveness of particles to resist crack growth in the intermediate stress intensity factor, can be rationalized as follows.

For an elastic-plastic material with a power law strain hardening, a crack growth model was derived involving mechanical, cyclic, fatigue properties as well as a length parameter associated with the microstructure, Ellyin (1986). The crack propagation model has the form of

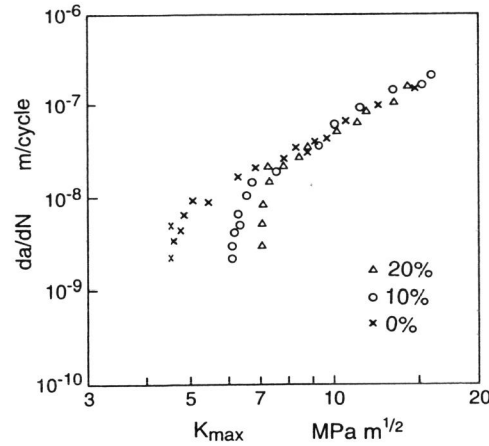


Fig. 4 Variation of the crack growth with the maximum stress intensity, K_{max} , at a load ratio of $R = -0.4$, for the 20% and 10% $Al_2O_3/6061$ Al composite and the 6061 aluminum alloy.

$$\frac{da}{dN} = 2\delta^* \left[\frac{\Delta K^2 - \Delta K_{th}^2}{4\psi E \sigma_f' \epsilon_f' \delta^*} \right]^{1/\beta} \quad (2)$$

where σ_f' , ϵ_f' are the fatigue strength and ductility coefficients and $\beta = -(b+c)$ with b and c appearing as the exponents in the Coffin-Manson fatigue life relationship, δ^* is a microstructural length parameter indicating the extent of 'process zone' and is generally of the order of the material grain size, and $\psi = \psi(n')$ is a parameter, function of cyclic strain hardening exponent, n' and depends on the chosen singularity fields, Ellyin (1986). The crack growth model (2) was obtained based on a material's capacity to absorb a certain amount of plastic strain energy. In the intermediate ΔK range, where ΔK_{th}^2 can be neglected compared to ΔK^2 , then (2) reduces to:

$$\frac{da}{dN} = 2\delta^* \left[\frac{\Delta K}{(4\psi E \sigma_f' \epsilon_f' \delta^*)^{1/2}} \right]^{2/\beta} \quad (3)$$

A number of empirically proposed crack growth models can be derived as a particular case of relation (3). It is interesting to note that for the aluminum alloy $2/\beta \approx 3.2$ and the slope of the straight line in Fig. 4 is 3.3.

Fine and Davidson (1983) have proposed an energy-based crack growth law

$$\frac{da}{dN} = \frac{A \Delta K^4}{G \sigma_y 2U} \quad (4)$$

where A is a constant, G is the shear modulus and U is an effective surface energy. For the matrix material, the constants in (4) can be determined by equating (3) and (4), see Ellyin (1996). The exponent 4 in eq. (4) over estimates the slope of the linear portion, therefore, we can write (4) in the form of

$$\frac{da}{dN} = \frac{A(\Delta K)^{2\beta}}{G \sigma_y 2U} \quad (5)$$

For a particle-reinforced composite, we may express U as

$$U_c = U_m(1 - f_a) + U_p f_a \quad (6)$$

where subscripts c , m and p refer to the composite, matrix and particle, respectively, and f_a is the area fraction of particles. Based on a uniform particle distribution

$$f_a = f_v^{2/3} \quad (7)$$

Substituting from (1), (7) and (6) into (5) and noting that $U_p \ll U_m$, the crack growth rate of the composite is given by

$$\left[\frac{da}{dN} \right]_c = \frac{A(\Delta K)^{2\beta}}{G_c \sigma_{ym} 2U_m [(1 + f_v^\alpha)(1 - f_v^{2/3})/C]} \quad (8)$$

The crack growth rate in the matrix alloy is similarly given by

$$\left[\frac{da}{dN} \right]_m = \frac{A(\Delta K)^{2\beta}}{G_m \sigma_{ym} 2U_m} \quad (9)$$

A comparison of the crack growth rate of the composite with that of the same length crack in the matrix alloy under the same ΔK , is obtained by dividing (8) into (9), which gives

$$\frac{(da/dN)_c}{(da/dN)_m} = \frac{1.14 G_m}{G_c [(1 + f_v^\alpha)(1 - f_v^{2/3})]} \quad (10)$$

The right-hand-side of (10) is approximately equal to 1, and thus, the growth rate of the composite approaches that of the matrix alloy, as seen in Fig. 4.

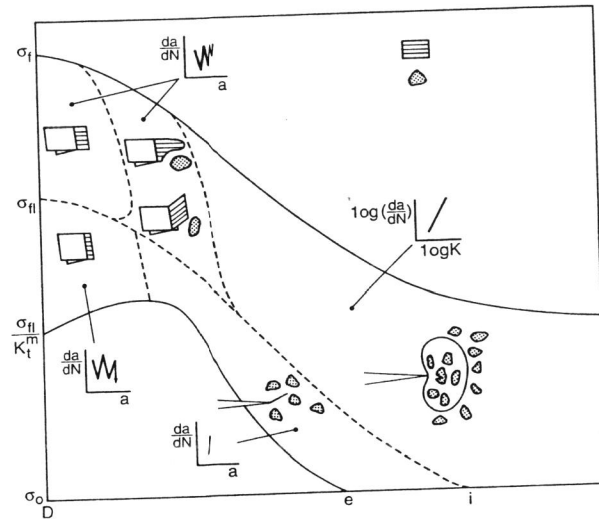


Fig. 5 Crack growth regimes for short crack (SG), pre-cess short crack (PCS), transition stage to long crack (ST), long crack (LG) and near threshold long crack (LT). The cyclic plasticity pattern ahead of different length cracks in the metal matrix composite is also depicted. The ordinate in the figure is the amplitude and the abscissa is the crack length.

CRACK-PHASE DIAGRAM OF PMMCS

Based on the observed behaviour of short and long cracks in particulate-reinforced composites, six crack growth regimes were identified by Li and Ellyin (1995a): unstable growth; long crack growth; near-threshold long crack growth; short crack growth; pre-cess short crack growth, and non-growth phases. Figure 5 combines all six phases in a diagram which displays the range of applied stress amplitude and crack length for each phase. Each phase boundary corresponds or is related to an overall material property.

(i) **The short crack growth, SG**, takes place at high stress amplitudes denoted on the ordinate by the fatigue limit σ_{fl} and the fracture stress σ_f , corresponding to a crack length of an average diameter particle D . (There is often a cracked particle in the composite due to manufacturing process). As the crack grows, the required applied stress to drive it decreases. The short crack growth rate, as discussed earlier, is local stress dominated as depicted by the da/dN vs. a , diagram at the top-left corner. These cracks generally grow along the slip bands, however, in the

PMMCs, both the size and shape of the crack-tip plastic zone is affected by the near by particle, as depicted in the figure by either bowing or branching of the crack tip plastic zone.

(ii) **The pre-cess short crack phase, PCS**, is bounded between the applied fatigue limit stress, σ_{fl} , and an applied stress of σ_{fl}/K_t^m where K_t^m is a local material stress concentration factor

$$K_t^m = \Delta\sigma_{loc}/\Delta\sigma_{appl}. \quad (11)$$

where $\Delta\sigma_{loc}$ is a local stress range averaged over a representative volume. With the increased crack length the influence of local stress decreases. σ_{fl}/K_t^m represents a local stress equal to the fatigue limit of the bulk material.

(iii) **Near-threshold long crack growth, LT**, is depicted in Fig. 5, by a growth characteristic which corresponds to lower stresses than those of short cracks but a longer length, and a very steep growth rate. The cracks in this zone generally propagated along a slip band in the matrix. The particles along the crack path generally tend to debond rather than crack. The lower boundary of this phase corresponds to the threshold condition

$$a_{th} = \frac{\Delta K_{th}^2}{(Y\Delta\sigma/2)^2}, \quad \frac{\Delta\sigma}{2} < \sigma_{fl} \quad (12)$$

where Y is a crack geometric factor.

(iv) **The long crack growth, LG**, phase is bounded at its upper boundary by the critical condition of unstable crack growth. This condition is governed by the material toughness, i.e. the critical stress intensity value determined from the resistance curve,

$$a_c = \frac{\Delta K_c^2}{(Y\Delta\sigma/2)^2}. \quad (13)$$

At higher values of stress, ΔK_c , is to be substituted by an elastic-plastic parameter.

At the long growth regime and intermediate ΔK , the plastic zone is of a multiple slip nature as shown in Fig. 5, lower right hand corner. The resistance of a particle to the crack advance depends on the cyclic plastic zone ahead of a nearby crack. At the threshold for the long crack growth, ΔK_{th} , the plastic zone (slip band) length is not long enough to extend over the neighbouring particle and to crack it.

In summary, each of the above crack growth phase boundaries correspond to a certain material property. In the case of short cracks, they are strength parameters in terms of stress, i.e. σ_f or σ_{fl} whereas for the long cracks they are related to the stress intensity factors e.g. ΔK_c or ΔK_{th} . The short crack regime in PMMC's is more extensive than that of the matrix alloy, and the

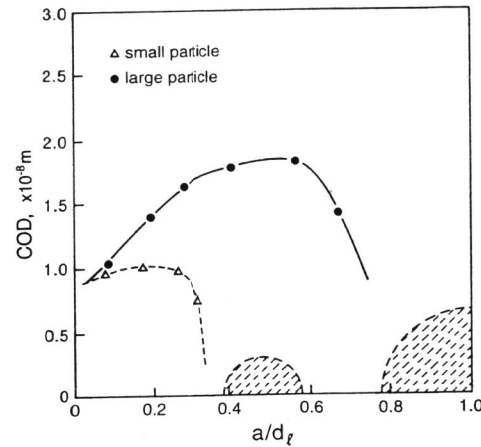


Fig. 6 Variation of crack opening displacement (COD) during a crack growth towards a particle in a fine composite (open triangles), compared with that in a composite with particles twice larger but with the same volume fraction and under the same loading condition (solid circles).

plastic zone shape varies as the crack tip approach a particle, as depicted in Fig. 5. Further discussion on the crack tip cyclic plasticity patterns can be found in Ellyin and Li (1995).

Effect of Particle Size

The effect of the particle size on the crack opening displacement, COD, of an advancing crack was investigated by Li and Ellyin (1994). A fine and a coarse particle-reinforced composite with the same volume fractions were analyzed. A comparison of the variation of COD as the crack approach a particle on its path, is shown in Fig. 6. In this figure the abscissa is non-dimensionalized by dividing the crack length, a , by the spacing between large particles, d_p . The ordinate is the crack opening displacement. It is seen that the effect of a particle on the advancing short crack is noticeable when the crack tip is very close to the particle. In the case of a coarse particle-reinforced composite, the crack growth is unimpeded for a longer distance. This figure clearly indicates that for the same applied load and volume fraction, a fine particle composite provide a better resistance to the short crack growth than a coarse particle one.

Crack tip stress is also influenced by the nearby particle size. For example, for the same short crack length and an equal distance from the crack tip, a larger particle reduces the crack tip stress more than a small one, and has a larger influence zone. The normal stress, however, is greater

in a large particle compared to a smaller one. For example, for a short crack of $a = 36 \mu\text{m}$ at a distance $d = 20 \mu\text{m}$ from a particle, the maximum stress at a $20 \mu\text{m}$ diameter particle is 4 times the applied stress, whereas it is 1.4 times the applied stress for a particle half the above size, Li and Ellyin (1994). Therefore, a large particle is more likely to fracture when a crack approaches it.

The fracture mechanism also changes from decohesion to particle cracking as the size of particle increases.

CONCLUSIONS

From the results presented above, the following conclusions are drawn:

Three types of damage: particle debonding, particle fracture and matrix cracking are primarily observed during cyclic loading of particle-reinforced metal matrix composites.

Initiated short cracks grow under the fatigue limit of the composite in a shear dominated mode with a drastically varying growth rate. A crack may reach a length of up to $400 \mu\text{m}$ before being arrested by the surrounding particles.

With the increased applied stress and crack length, the microstructure sensitivity decreases, and a transition from a single slip band to a multiple slip plastic zone occurs.

A crack-phase diagram for PMMC's is presented. It shows the range of applied stress and crack length for different crack growth mechanisms. The boundaries of each phase correspond to the overall material properties, and depict a certain state of crack-tip cyclic plastic zone.

The particle size plays an important role in reducing the crack tip stress/strain and crack tip opening displacement. There is a transfer of the maximum stress location from the crack tip to a nearby large particle, as the crack approaches the particle.

ACKNOWLEDGEMENT

This paper was prepared while the author was a visiting professor at the Ecole Nationale Supérieure d'Arts et Métiers (LAMEF-ENSAM) Bordeaux, France. The ambience and facilities provided by Professor Jean-Luc Lataillade was greatly appreciated. The work reported here is supported by a strategic grant from the Natural Sciences and Engineering Research Council of Canada (NSERC). The contribution of Dr. Chingshen Li in obtaining the initial results is hereby acknowledged.

REFERENCES

- Duralcan Company (1993). Manufacturer's Data, San Diego, CA.
- Ellyin, F. (1986). Crack growth rate under cyclic loading and effect of different singularity fields. *Engng. Fract. Mech.*, **25**, pp. 463-473.
- Ellyin, F. and C.-S. Li (1995). The role of cyclic plasticity in crystallographic crack growth retardation. *Mater. Sci. Res. Int. (JSMS)*, **1**, pp. 137-143.
- Ellyin, F. (1996). *Fatigue Damage, Crack Growth and Life Prediction*. Chap. 7, Chapman & Hall, London.
- Fine, M.E. and D.L. Davidson (1983). Quantitative measurement of energy associated with a moving fatigue crack. *ASTM STP*, **811**, pp. 350-368.
- Li, C.-S. and F. Ellyin (1994). Short crack trapping/untrapping in particle-reinforced metal-matrix composites. *Composite Sci. Technol.*, **52**, pp. 117-124.
- Li, C.-S. and F. Ellyin (1995a). On crack phases of particulate-reinforced metal matrix composites. *Fatigue Fract. Engng. Mater. Struct.*, **18**, pp. 1299-1309.
- Li, C.-S. and F. Ellyin (1995b). Short crack growth behaviour in a particulate-reinforced aluminum alloy composite. *Metall. Trans.*, **26A**, pp. 3177-3182.
- Li, C.-S. and F. Ellyin (1996). Fatigue damage and its localization in particulate metal composites. *Mater. Sci. Engng. A*, (in press).
- Lloyd, D.J. (1994). Factors influencing the tensile ductility of melt processed particle reinforced aluminum alloys. In: *Intrinsic and Extrinsic Fracture Mechanisms in Inorganic Composite Systems* (eds. J.J. Lewandowski and W.H. Hunt, Jr.), TMS Publ., pp. 39-47.
- Shang, J.K. and R.O. Ritchie (1989). On the particulate-size dependence of fatigue crack propagation thresholds in SiC particulate reinforced aluminum-alloy composites: role of crack closure and crack trapping. *Acta Metall.*, **37**, pp. 2267-78.